RSC Advances

PAPER

View Article Online
View Journal | View Issue

Cite this: *RSC Adv.*, 2021, **11**, 33354

Enhancement of thermal and mechanical properties of silicone rubber with γ-ray irradiation-induced polysilane-modified graphene oxide/carbon nanotube hybrid fillers

Ke Cao,[a] Bolong Li,[b] Yang Jiao,[a] Yongjun Lu,[a] Liancai Wang,[a] Yueying Guo[a] and Pei Dai*[a]

In this study, a polysilane-modified graphene oxide (GO) and carbon nanotube (CNT) nanocomposite (GO/CNTs-Si) was prepared as a thermal conductive nanofiller to enhance the thermal and mechanical properties of silicone rubber composites. By γ-ray-radiation 3-methacryloxypropyltrimethoxy silane (MPTMS) was polymerized on the surface of GO and CNTs to improve the interfacial interaction between the GO/CNTs-Si and SR matrix. FTIR characterization results demonstrated that polysilane modified the GO/CNTs successfully. The pristine GO/CNTs and resultant GO/CNTs-Si were individually incorporated into α,ω-dihydroxypolydimethylsiloxane to vulcanize SR composites. Compared with SR–GO/CNTs, SR–GO/CNT-Si exhibited better mechanical and thermal performance. Moreover, the time-dependent complex modulus of SR–GO/CNTs-Si was much higher than that of SR–GO/CNTs, which indicates longer service time and more stable performance. In terms of electronic packaging, SR–GO/CNTs exhibited better performance than the 1180B counterpart. The low value of warpage of chip packaged by SR–GO/CNTs implied that SR–GO/CNTs-Si could have potential application as the thermal interface electronic packaging material.

Received 12th July 2021
Accepted 10th September 2021

DOI: 10.1039/d1ra05340j

rsc.li/rsc-advances

Introduction

Silicone rubber (SR), due to its properties such as high thermal stability, elasticity and electric insulation, can be used as the thermal interfacial material of heat transmitting and radiating parts in various fields, such as aviation, electronics and machinery manufacturing.[1,2] With the rapid development of miniaturization and integration of electronics, the removal of excess heat and the interfacial stresses have become increasingly critical issues for the enhancement of device service life.[3] In order to overcome the disadvantages of thermal conductivity and mechanical properties of pure silicone rubber, fillers can be incorporated to the material.[4,5] Various types of nano-materials such as silver nanowires,[6] ZnO nanograins,[7] aluminum nitride nano-sheets,[5,8] boron nitride nano-sheets,[9,10] carbon nanotubes and graphene nanosheets[11,12] have been developed as functional fillers to improve the thermal, mechanical, electrical and other properties of SR-based composites.[13]

Among these fillers, carbon nanotubes (CNTs) and graphene nanosheets as the carbon nanomaterials possess remarkable physical and chemical properties arising from its extraordinary mechanical strength, large specific surface area, high intrinsic mobility and excellent thermal and electrical conductivities.[14–16] Moreover, it has been shown that a combination of graphene and CNTs can endow outstanding performances for improving the properties of nanocomposites. Jyoti[17] prepared a graphene oxide/CNT hybrid material, which reinforced acrylonitrile butadiene styrene (ABS). The static and dynamic mechanical properties of graphene oxide/CNT ABS hybrid composites were significantly improved. Not only the mechanical properties but the tribological properties were remarkable due to the incorporation of hybrids of graphene oxide and CNTs.[18] Furthermore, the hybrid carbon nanomaterials can be also employed as advanced functional materials. Chen[19] synthesized polydopamine-functionalized graphene/CNTs as the adsorbent to measure the polycyclic aromatic hydrocarbons. However, CNTs and graphene are both difficult to disperse in the polymer matrix during processing, and they are not suitable for industrial-scale production because of the over complicated technology and expensive cost.[20]

Modifying carbon nanomaterials by γ-ray exhibits great advantages, such as easy control, cost-effectiveness and environmentally friendly, which show the potential to be scaled up.[21–23] Recently, hybrid carbon nano-filler systems have been investigated as a new approach to enhance the performance of composites.[24,25] Moreover, the incorporation of graphene/CNT

[a]*Beijing Key Laboratory of Radiation Advanced Materials, Beijing Research Center for Radiation Application, Beijing 100015, People's Republic of China. E-mail: daipei008@126.com*

[b]*Beijing Radiation Center, Beijing 100875, China*

hybrid fillers prepared by γ-ray radiation into a rubber matrix results in favorable dispersion and significant improvement in the properties.[26–28] The mechanical properties and thermal stability of poly(vinyl alcohol) composite films were enhanced since the interconnected 3D structure of graphene/CNTs formed that inhibited the aggregation.[29] The irradiation technique has opened a sane path for the preparation of graphene/CNTs hybrid fillers with good dispersibility.

In this study, functionalized graphene oxide/carbon nanotube hybrid fillers (GO/CNT-Si) were synthesized in a facile way. The oxygen functional groups of GO and CNT were induced to produce oxygen radical, which initiated 3-methacryloxypropyltrimethoxy silane polymerized on the surface of GO and CNT. SR and GO/CNT-Si were mixed by mechanical stirring and molded by casting. The GO/CNT-Si hybrid carbon nanomaterial could significantly improve the thermal transfer ability and mechanical properties of SR owing to the interconnected structure.

Experiment

Materials

Graphene oxide was obtained from The Sixth Element (Changzhou) Materials Technology Co., Ltd, China. Multi-walled carbon nanotubes (purity > 95 wt%) with an average length of 1–2 μm were purchased from Chengdu Organic Chemistry Co., Ltd, China. 3-Methacryloxypropyltrimethoxy silane was purchased from Shanghai Macklin Biochemical Co., Ltd, China. α,ω-Dihydroxy polydimethylsiloxane (PDMS) with viscosity of 50 Pa s was purchased from Hoshine Silicon Industry Co., Ltd, Luzhou, China, and was used as received. Tetraethyl orthosilicate used as the cross-linking agent and dibutyltin dilaurate used as the catalyst were purchased by Fuchen Chemical Reagent Co., Ltd, Tianjin, China. The underfill 1180B as the reference warpage sample is one kind of commercial primer applied between chip and substrate. It was purchased from Themis Industrial Adhesives. All the other chemical reagents (analytical grade) were obtained from Beijing Chemical Works (China) and used as received without further purification.

Characterization and measurement

The morphology of GO/CNT-Si was characterized *via* high-resolution transmission electron microscopy (HRTEM, Tecnai F30, Philips-FEI Co., Holland). The vulcanized SR composite samples were fractured in liquid nitrogen, then the fractured surface was sputtered with gold, and the fractured morphologies of the samples were observed by scanning electron microscopy (SEM; model JCM-5000, Jeol Co., Japan).

The cross-linking degree was determined by the gel content percentage of the sample, which was extracted in THF at the boil for 72 h. The cross-linking degree (CD) can be calculated from weight of gel of composite sample according to eqn (1)

$$\mathrm{CD} = \frac{m_2}{m_1} \times 100\% \quad (1)$$

where m_2 indicates the weight of the gel of sample and h_1 indicates the original weight of the sample before solvent (THF) extraction. Five samples were tested for each SR–GO/CNT-Si-*XX*, and the average values of the gel content test results are presented for comparison and analysis.

The tensile properties of the SR composite were measured by a SANS CMT-4203 universal mechanical tester with a load cell of 100 N and a gauge length of 20 mm at across the head speed of 10 mm min^{-1}.

Thermal expansion performance was tested on a thermo-mechanical analyzer (Shimadzu TMA-50, Shimadzu, Japan). The sample (5 mm × 5 mm) were heated in the temperature range from 60 °C to 200 °C at a heating rate of 5 °C min^{-1} under N_2. The thermal expansion ratio (TER) can be calculated from the increased thickness of the SR composite sample according to eqn (2)

$$\mathrm{TER} = \frac{h_2}{h_1} \times 100\% \quad (2)$$

where h_2 is the thickness of the sample at different temperatures and h_1 is the original thickness of the sample.

Thermogravimetric analysis (TGA) was carried out on a Shimadzu TGA-50 thermal analyzer. The samples were heated from room temperature to 800 °C at a heating rate of 10 °C min^{-1} under N_2. Thermal conductivity of the samples was obtained on a DZDR-S thermal conductivity tester (Nanjing Dazhan Institute of Electromechanical Technology) by the standard method (isotropic), which was based upon a transient plane source technology. Viscoelastic properties of the cured SR composites were measured *via* time–temperature superposition experiments using a GABO Eplexor 500 N dynamic mechanical thermal analyzer under tensile mode operation. The temperature frequency sweep method was employed since viscoelastic properties are both time- and temperature-dependent. The temperature was increased from −140 °C to −30 °C with the frequency scanned at 1, 3, 10, and 50 Hz at each isothermal temperature. The uncured packaging underfill filled the IC chip (14 mm × 14 mm) from side to side at room temperature. The chip warpage measurement was carried out on a Quantigraf-600 system (C&B Tech., USA) with temperature increasing from 25 °C to 150 °C then decreasing to 25 °C.

Synthesis of polysilane-functionalized GO/CNT nanocomposites

GO/CNT nanocomposites were synthesized by γ-ray radiation in a typical procedure: 500 mg GO and 500 mg CNT were dispersed into a glass flask with 50 mL of tetrahydrofuran (THF) by ultrasonication on a scientz-II Dultrasonicator (Ningbo, China) at room temperature for 1 h to obtain a uniform suspension. The 50 mL 3-methacryloxypropyltrimethoxy silane was dropped in the THF suspension of GO/CNTs with evenly stirring. The THF/3-methacryloxypropyltrimethoxy suspension of GO/CNTs was transferred into a glass tube. Then, the mixture was directly exposed to γ-ray from a ^{60}Co source in air. The absorbed dose was 50 kGy at a dose rate of about 50 Gy min^{-1}. The suspension was filtrated-washed with THF for five times to remove homopolymeried polysilane and unreacted silane, and then dried for 12 h in a vacuum oven at 60 °C. The production was named GO/CNT-Si.

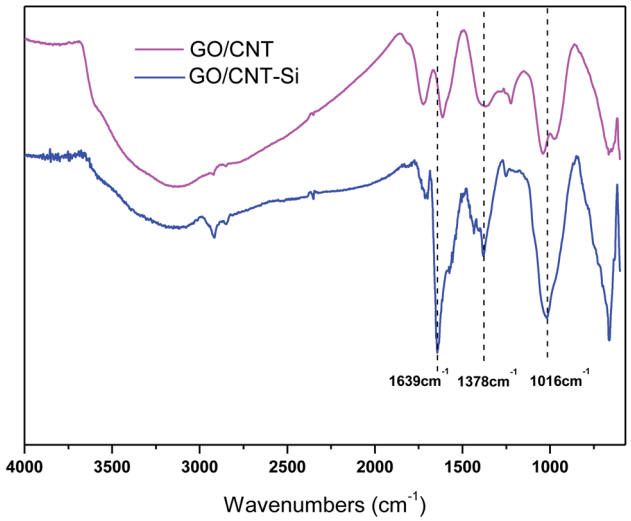

Fig. 1 FTIR spectra of GO/CNT and GO/CNT-Si.

Preparation of the SR–GO/CNT-Si composite

A SR–GO/CNT-Si composite was prepared by solution blending. First, PDMS (60 g), catalyst (1 g) and cross-linking agent (5 g) were mixed under mechanical stirring at room temperature for 10 min. Then, GO/CNT-Si powder with different weights was dispersed in THF (20 mL) by an ultrasonicator for 30 min to obtain uniform dispersion. The GO/CNT-Si THF suspension was dropped in the PDMS mixture under stirring. Finally, the mixed solution was poured into a Teflon mold for sample formation (150 mm × 150 mm × 2 mm). The formation mold containing sample was placed in an oven, and the sample was cured at 25 °C. A series of SR composite samples with different GO/CNT-Si loadings were prepared in the same way and named SR–GO/CNT-Si-*XX*, where *XX* represent the weight percentage of GO/CNT-Si to PDMS.

Result and discussion

Fig. 1 shows the FTIR spectra of GO/CNTs and GO/CNT-Si. The broad absorption of ~3200 cm^{-1} can be assigned to the O–H vibration.[30] The strong peak at 1639 cm^{-1} was attributed to the stretching vibration of C=C.[31] After radiation of GO/CNTs in the MPTMS/THF solution, the strong absorption band at 1016 cm^{-1} attributed to the stretching vibration of Si–O appeared, which obscured the C–O stretching vibrational absorption. The signal at 1378 cm^{-1} was assigned to the $-CH_3$ stretching vibration of polysilane. Together, these results confirmed that MPTMS was successfully graft-polymerized on the surface of graphene/CNT nanocomposites.

The TEM micrographs of the pristine CNTs, GO and modified GO/CNT-Si are shown in Fig. 2. The frizzy CNT aggregation

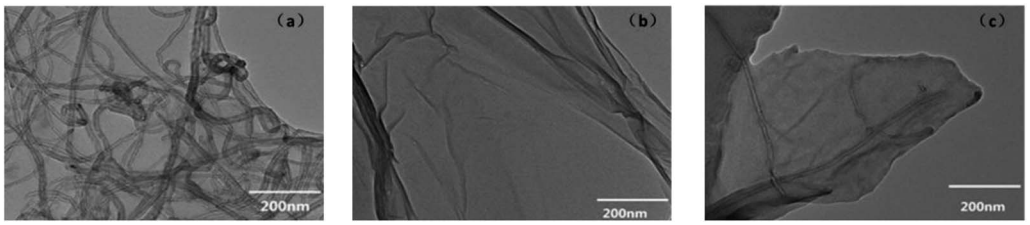

Fig. 2 TEM images of (a) pure CNTs, (b) pure GO and (c) GO/CNT-Si.

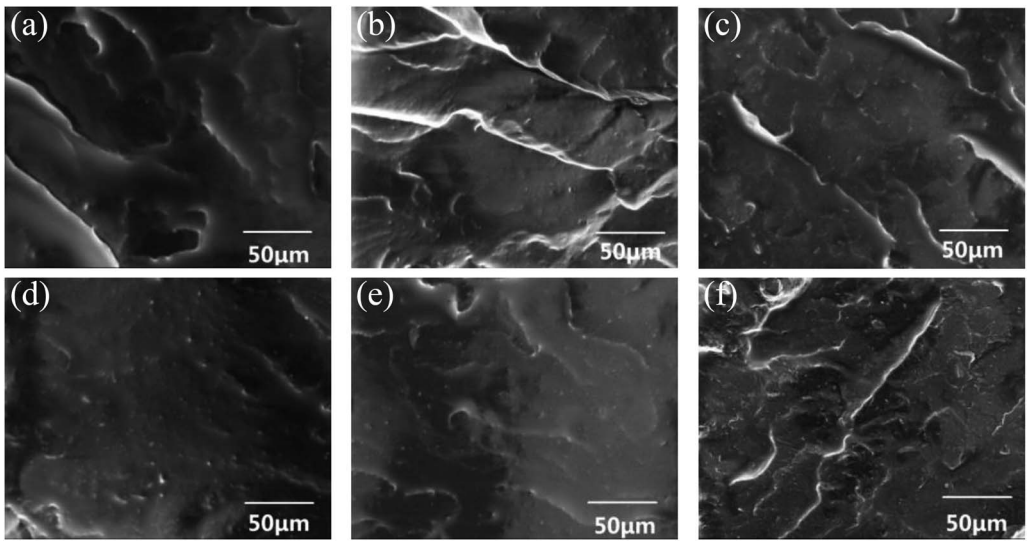

Fig. 3 SEM images of fractured surface of (a) SR–GO/CNT-Si-0.1, (b) SR–GO/CNT-Si-0.5, (c) SR–GO/CNT-Si-1.0, (d) SR–GO/CNT-Si-1.5, (e) SR–GO/CNT-Si-2.0 and (f) SR–GO/CNT-Si-3.0 composites.

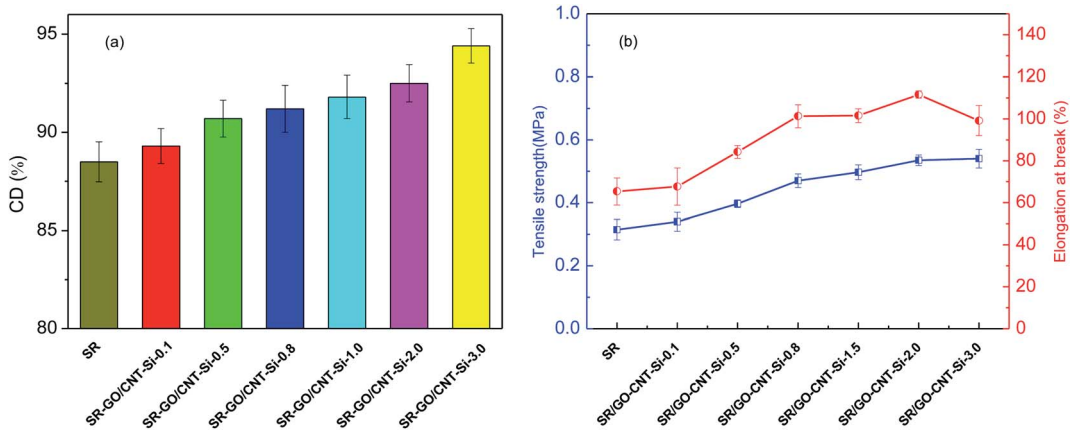

Fig. 4 Cross-linking degree (a), tensile strength and the elongation at break (b) of SR and SR composites with different GO/CNT-Si contents.

dispersed on the micro grid support membrane. The micrographs of GO/CNT-Si exhibited that the CNTs dispersed individually on the surface and edges of graphene nanosheets. CNTs are uniformly distributed between the layers of graphene nanosheets, which indicated the formation of the interconnected 3D network structure.[32] The structure could effectively avoid the aggregation of nanotubes and nanosheets. Furthermore, it might make GO/CNT-Si suitable for preparing SR nanocomposites with good thermal conductivity.

The distribution of GO/CNT-Si in the SR matrix was investigated by observing the morphology of the fractured surface of each composite sample. SEM micrographs of SR–GO/CNT-Si-0.1, SR–GO/CNT-Si-0.5, SR–GO/CNT-Si-1.0, SR–GO/CNT-Si-1.5, SR–GO/CNT-Si-2.0 and SR–GO/CNT-Si-3.0 composites are shown in Fig. 3(a)–(f). SEM images clearly show that GO/CNT-Si was dispersed homogeneously in the SR matrix. As the weight percentage of GO/CNT-Si increases, more and more nanofiller particles appeared on the fracture surface. The homogeneous dispersion of GO/CNT-Si throughout the SR matrix would help improve the mechanical properties and thermal transfer ability.

The relative amount of CD can provide useful information on cross-linking efficiencies. Fig. 4(a) shows the CD of SR–GO/CNT-Si-*XX* determined experimentally as a function of the GO/CNT-Si content. As expected, the CD was increased from 88.5% to 94.4% with the increase in the GO/CNT-Si weight percentage from 0.1 wt% to 3.0 wt%. Compared with SR, SR–GO/CNT-Si was higher due to cross-linking between the fillers and the matrix. Meanwhile, CD was one of the important factors which improved mechanical performances of SR–GO/CNT-Si significantly. Increasing the addition amount of GO/CNT-Si could lead to a considerable increase in the tensile strength of SR. Besides the development of CD, GO and CNT are both rigid reinforcement nanofillers, which formed interactions with the SR matrix. Moreover, the good dispersal ability of GO/CNT-Si in SR contributed to the improvement of the mechanical properties. It can be concluded that the incorporation of GO/CNT-Si could simultaneously enhance the strength and toughness of SR–GO/CNT-Si composites. However, the negative effect for elongation at break of SR–GO/CNT-Si did not appear until the GO/CNT-Si content reached 3.0 wt%. This is mainly because the interaction between polysilane-modified GO/CNT-Si and SR matrix could reduce crack or defect under stress.

The operation of miniaturized and integrated electric devices would produce heat rapidly and intensively.[33] The thermal properties of SR packaging composites indicate that thermal expansion and thermal stability directly affect the

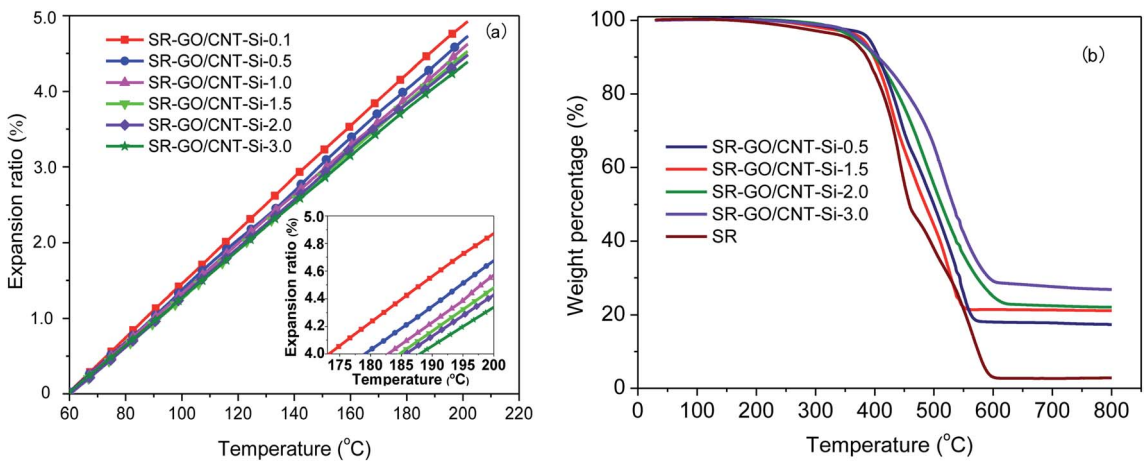

Fig. 5 The expansion ratio (a) and TGA curves (b) of SR composites with different GO/CNT-Si contents.

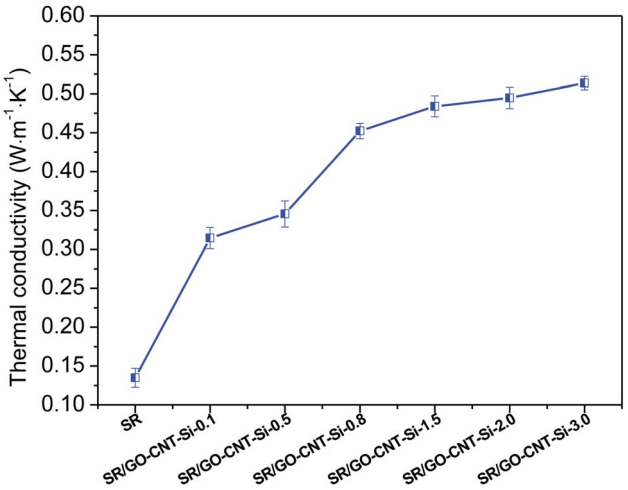

Fig. 6 Thermal conductivity of SR composites with different GO/CNT-Si contents.

service life of electronic equipment. The polymer chain thermal motion depends on temperature, so that the thermal expansion ratio has the positive correlation with temperature.[34] As shown in Fig. 5(a), the thermal expansion ratio of SR–GO/CNT-Si nanocomposites increased with the increase in temperature. On other hand, it decreased with the increase in the GO/CNT-Si content. The TER of SR–GO/CNT-Si-0.1 rose to 4.85% from 60 °C to 200 °C. SR–GO/CNT-Si-3.0 with more GO/CNT-Si weight percentage exhibited lower thermal expansion ability. TER of SR–GO/CNT-Si-3.0 was 4.37%, which was lower than that of SR–GO/CNT-Si-0.1. The thermal expansion ratio of GO and CNTs is much lower than that of SR. The strong interaction of GO/CNT-Si and the SR matrix limited and restricted the thermal expansion motion of SR chains. At a high temperature, the low thermal expansion ratio of the composites could reduce the thermal stress, which led to the interfacial seal failure between the electronic device and SR.

As the temperature continued to rise, the covalent bond of the SR chain was vibrated more intensely and even broken. TGA was employed to investigate the thermal stability of SR/GO–CNT-Si composites. The pristine SR degradation curve included three weight loss stages. The temperature zone of the first thermal degradation stage is from 158 °C to 360 °C. The weight loss is attributed to the decomposition of the catalyst. The second weight loss stage with an initial temperature 360 °C and final temperature 462 °C was assigned to the unreacted –OH of SR chain.[35] The last stage (462–607 °C) was attributed to the degradation of main chain of SR.[36] As shown in Fig. 5(b), the initial temperature of SR/GO–CNT-Si was increased except for the catalyst weight loss stage with the incorporation of more GO–CNT-Si. Moreover, the char yield of SR/GO–CNT-Si also increases with the increase in the GO–CNT-Si content. The results evidenced that the hybrid carbon nanofiller could improve the heat resistance of SR composites. The temperature of the maximum mass loss rate of SR/GO–CNT-Si-3.0 was nearly 50 °C higher than that of SR. The combined survey results from the thermal expansion and thermal stability tests concluded that GO–CNT-Si could improve the thermal properties of SR for the application in electronic packaging.

Thermal conductivity is the key factor for electronic packaging thermal interface materials. The SR composites should form an interconnected thermal conductive network to transfer heat rapidly. The polysilane on the GO/CNT-Si surface improved the dispersibility and compatibility with the SR matrix, which reduced the thermal resistance between GO/CNT-Si and SR, so that the thermal conductivity of SR composites increased with the increase in the GO/CNT-Si content (Fig. 6). The maximum value of GO composites is 0.51 W m^{-1} K^{-1} (SR–GO/CNT-Si-3.0), which is nearly 4-fold higher than that of neat SR. On the one hand, the modified GO/CNT dispersed uniformly in SR. On the other hand, GO as a 2-D carbon nanomaterial and CNT as a 1-D carbon nanomaterial could connect with each other to form a 3-D thermal transfer network. It has been reported that the thermal conductivity of the SR composite is 0.26 W m^{-1} K^{-1} with 8 wt% graphene nanoplatelet addition.[37] In our study, the thermal conductivity of the SR composite reached 0.31 W m^{-1} K^{-1} with only a tiny amount of GO/CNT-Si (0.1 wt%).

Stress relaxation of the electronic packaging material can greatly affect its application performance. SR is one of the viscoelastic polymer packaging materials and its viscoelastic properties were estimated *via* the time–temperature superposition (TTS) principle.[38,39] The right part of Fig. 7(a) with the

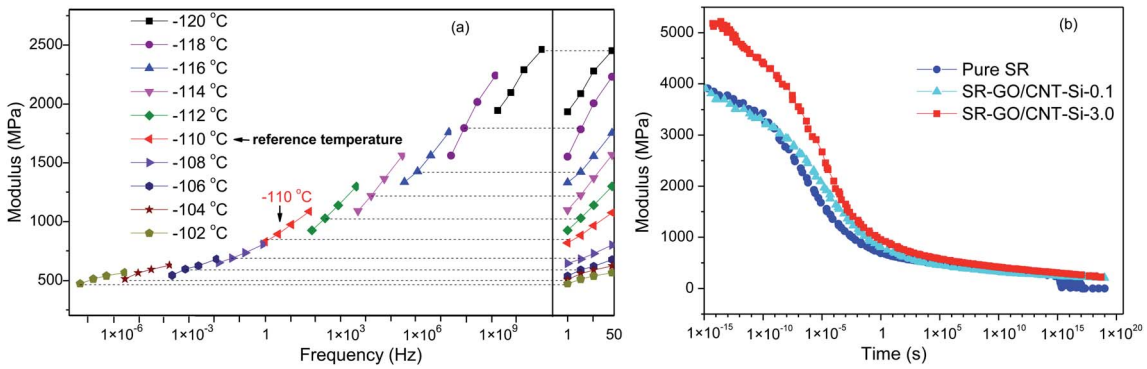

Fig. 7 (a) Frequency dependence of the complex modulus of a cured pure SR at different isothermal temperatures. (b) Fitted master curves of stress relaxation generated by shifting the complex modulus curves using the TTS principle with respect to a reference temperature of −110 °C.

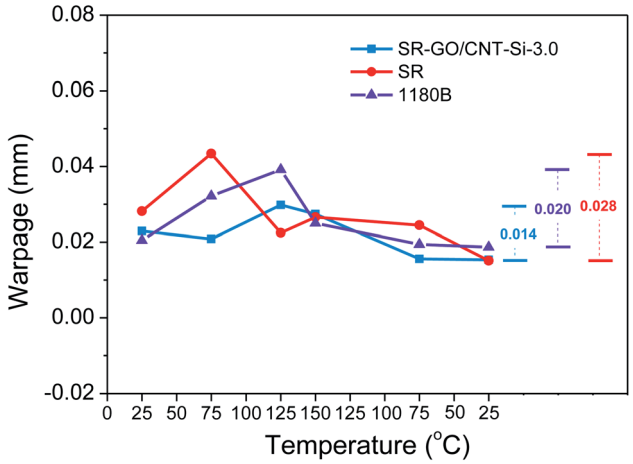

Fig. 8 The warpage of SR, SR–GO/CNT-Si-3.0 and 1180B (Themis) at different temperatures.

frequency range from 1 to 50 Hz is the TTS plot of SR. These showed the frequency dependence of the complex modulus of SR at different isothermal temperatures from −120 °C to −102 °C. Based on this figure, a modulus curve of a certain temperature (*e.g.*, −110 °C) was selected as the reference. Then, this modulus curve can be extended to a lower frequency range by shifting the higher temperature modulus curves to the left along the frequency axis, and *vice versa*. Thus, a master curve can be constructed for that reference temperature over an extended frequency range.

As shown in Fig. 7(a), the master curves of stress relaxation of pure SR were constructed by shifting the isothermal curves horizontally. After curve fitting, the master curves of the time-dependent stress relaxation modulus of SR composites are displayed in Fig. 7(b). The incorporation of GO–CNT-Si carbon nanocomposites improved the resistance ability to stress relaxation. Moreover, the modulus increased with the increase in the content of GO–CNT-Si in the SR composite. As the Fig. 7(b) shown, the modulus of pure SR was dropped to nearly zero obviously after 1×10^{15} s, whereas the modulus of SR/GO–CNT-Si-3.0 composites remained to 300 MPa. It proved that SR/GO–CNT-Si composites keep well useable performance.

In terms of electronic packaging, SR–GO/CNT-Si-3.0, SR and 1180B were applied as underfill between gaps of three flip-chip samples, respectively. Warpage of chips during the temperature cycling (25 °C–150 °C–25 °C) was measured. Warpage is the difference between the maximum and the minimum distances of the median surface of chips from the reference plane, where the reference plane is determined through the least-square method. It was obvious that the warpage of the chip used SR as an underfill is the largest, which was 0.043 mm at 75 °C and had a variation of 0.028 mm during the temperature cycling. Among three samples, the warpage of the chip where SR–GO/CNT-Si-3.0 was applied as an underfill is the smallest and its variation (0.014 mm) during the temperature cycling is also smaller than 1180B (0.020 mm). It was concluded that using SR-GO/CNT-Si-3.0 as an underfill can improve the thermo-mechanical reliability of flip-chips (Fig. 8).

Conclusion

In this study, the modified GO/CNT was designed and prepared by MPTMS grafting polymerization induced by γ-ray irradiation. The produced GO/CNT-Si exhibited better dispersion and interfacial interaction with the SR matrix. As expected, the mechanical properties of SR–GO/CNT-Si increased with the increase in the carbon nanocomposite content. The thermal properties including thermal expansion ratio, thermal stability and conductivity were improved significantly, which is an important criterion for the significant enhancement in thermal interface electronic packaging performances of the composites. The incorporation of GO/CNT-Si could prolong the service life of SR composite due to the resistance ability to stress relaxation. It is concluded that using SR–GO/CNT-Si as underfill can improve the thermo-mechanical reliability of flip-chips.

Conflicts of interest

There are no conflicts to declare.

Acknowledgements

This study was funded by National Natural Science Foundation of China (11805016) and Beijing Nova Program (Z201100006820113).

References

1 Y. L. Li, M. J. Li, M. L. Pang, S. Y. Feng, J. Zhang and C. Q. Zhang, *J. Mater. Chem. C*, 2015, **3**(21), 5573–5579.
2 A. Ba, A. Kovalenko, C. Aristégui, O. Mondain-Monval and T. Brunet, *Sci. Rep.*, 2017, **7**, 40106.
3 J. N. Song, C. B. Chen and Y. Zhang, *Composites, Part A*, 2018, **105**, 1–8.
4 T. Chen and B. Liu, *Chem. Phys. Lett.*, 2018, **693**(1), 121–126.
5 J. W. Zha, Z. M. Dang, W. K. Li, Y. H. Zhu and G. Chen, *IEEE Trans. Dielectr. Electr. Insul.*, 2014, **21**(4), 1989–1996.
6 P. Lu, Z. M. Qu, Q. G. Wang, L. Y. Bai and S. Y. Zhao, *IOP Conf. Ser.: Mater. Sci. Eng.*, 2018, **301**, 012052.
7 R. Suntako, *Appl. Mech. Mater.*, 2018, **878**(1), 281–285.
8 Q. H. Mu, D. Peng, F. Wang, J. H. Li and S. Zhang, *Mater. Sci. Forum*, 2018, **926**(1), 45–50.
9 S. Kemaloglu, G. Ozkoc and A. Aytac, *Thermochim. Acta*, 2010, **499**, 40–47.
10 J. W. Gu, X. D. Meng, Y. S. Tang, Y. Li, Q. Zhuang and J. Kong, *Composites, Part A*, 2017, **92**, 27–32.
11 L. Gan, S. M. Shang, C. W. M. Yuen, S. X. Jiang and N. M. Luo, *Composites, Part B*, 2015, **69**, 237–242.
12 Y. Huang, X. Y. He, L. Gao, Y. Wang, C. X. Liu and P. Liu, *J. Mater. Sci.: Mater. Electron.*, 2017, **28**(13), 9495–9504.
13 M. T. Chen, T. Tao, L. Zhang, W. Gao and C. Z. Li, *Chem. Commun.*, 2013, **49**(16), 1612–1614.
14 Z. D. Han and A. Fina, *Prog. Polym. Sci.*, 2011, **36**(7), 914–944.
15 A. A. Balandin, S. Ghosh, W. Z. Bao, I. Calizo, D. Teweldebrhan, F. Miao and C. N. Lau, *Nano Lett.*, 2008, **8**(3), 902–907.

16 A. A. Balandin, *Nat. Mater.*, 2011, **10**(8), 569–581.
17 J. Jyoti, A. S. Babal, S. Sharma, S. R. Dhakate and B. P. Singh, *J. Mater. Sci.*, 2018, **53**(4), 2520–2536.
18 C. Min, D. Liu, C. Shen, Q. Zhang, H. Song, S. Li, X. Shen, M. Zhu and K. Zhang, *Tribol. Int.*, 2018, **117**(1), 217–224.
19 K. Chen, R. R. Jin, C. Luo, G. X. Song, Y. M. Hu and H. Cheng, *J. Sep. Sci.*, 2018, **41**(8), 1847–1855.
20 V. Kumar, J. Y. Lee and D. J. Lee, *Polym. Int.*, 2017, **66**(3), 450–458.
21 Y. Shi, D. Xiong, J. Li and N. Wang, *J. Phys. Chem. C*, 2016, **120**(34), 19442–19453.
22 J. Li, B. Zhang, L. Li, H. Ma and M. Yu, *Radiat. Phys. Chem.*, 2014, **94**, 80–83.
23 Y. W. Zhang, H. L. Ma, Q. L. Zhang, J. Peng, J. Q. Li, M. L. Zhai and Z. Z. Yu, *J. Mater. Chem.*, 2012, **22**(26), 13064–13069.
24 W. Fan, L. S. Zhang and T. X. Liu, *SpringerBriefs in Green Chemistry for Sustainability*, ed. S. K. Sharma, Springer, Dordrecht, 1st edn, 2017, Graphene-Carbon Nanotube Hybrids for Energy and Environmental Applications, pp. 53–90.
25 H. S. Kim, S. K. Lee, M. Wang, J. Kang, Y. Sun, J. W. Jung, K. Kim, S. M. Kim, J. D. Nam and J. Suhr, *Nanomaterials*, 2018, **8**(9), 694.
26 Y. Srinivasarao, S. Bashaiah, J. Abraham, K. C. James Raju, K. Nandakumar and T. Sabu, *J. Polym. Res.*, 2015, **22**(7), 137.
27 L. Valentini, S. B. Bon and N. M. Pugno, *Adv. Funct. Mater.*, 2017, **27**(24), 1606526.
28 L. Valentini, S. B. Bon, M. Hernández, M. A. Lopez-Manchado and N. M. Pugno, *Compos. Sci. Technol.*, 2018, **166**, 109–114.
29 X. G. Qi, J. Wang, J. Yang and G. Y. Liu, *China Synth. Rubber Ind.*, 2007, **6**, 450–453.
30 Z. H. Mo, Z. Luo, Q. Huang, J. P. Deng and Y. X. Wu, *Appl. Surf. Sci.*, 2018, **440**(1), 359–368.
31 W. L. Wu and J. Wang, *Silicon*, 2018, **10**(5), 1903–1910.
32 H. L. Ma, L. Zang, Y. W. Zhang, S. J. Wang, C. Sun, H. Y. Yu, X. M. Zeng and M. L. Zhai, *Radiat. Phys. Chem.*, 2016, **118**, 21–26.
33 J. Rasco, J. Een and W. Crooijmans, *US Pat.*, 20110203631A1, 2011.
34 S. Mohamadi, N. Sharifi-Sanjani and A. Foyouhi, *J. Polym. Res.*, 2013, **20**(1), 46.
35 W. S. Ma, J. Li, B. J. Deng, X. D. Lin and X. S. Zhao, *J. Wuhan Univ. Technol., Mater. Sci. Ed.*, 2013, **28**(1), 127–131.
36 O. K. Park, J. Y. Hwang, M. Goh, J. H. Lee, B. C. Ku and N. H. You, *Macromol*, 2013, **46**(9), 3505–3511.
37 Y. Z. Song, J. H. Yu, L. H. Yu, F. E. Alam, W. Dai, C. Y. Li and N. Jiang, *Mater. Des.*, 2015, **88**, 950–957.
38 S. C. Kwang, *Viscoelasticity of Polymers*, ed. S. C. Kwang, Springer, Dordrecht, 1st edn, 2016, Time-Temperature Superposition, pp. 437–457.
39 Y. He, *Thermochim. Acta*, 2005, **439**, 127–134.